

## ARA9 Modifies Agonist Signaling through an Increase in Cytosolic Aryl Hydrocarbon Receptor\*

(Received for publication, July 29, 1999, and in revised form, October 27, 1999)

John J. LaPres, Edward Glover, Elizabeth E. Dunham, Maureen K. Bunger, and Christopher A. Bradfield‡

From the McArdle Laboratory for Cancer Research, University of Wisconsin Medical School, Madison, Wisconsin 53706

The aryl hydrocarbon receptor (AHR) is a ligand-activated transcription factor that mediates the effects of agonists like 2,3,7,8-tetrachlorodibenzo-*p*-dioxin. In the current model for AHR signaling, the unliganded receptor is found in the cytosol as part of a complex with a dimer of the 90-kDa heat shock protein and an immunophilin-like molecule, ARA9. In yeast, expression of ARA9 results in an increase in the maximal agonist response and a leftward shift in the AHR dose-response curve. To better understand the mechanism by which ARA9 modifies AHR signal transduction, we performed a series of coexpression experiments in yeast and mammalian cells. Our results demonstrate that ARA9's influence on AHR signaling is not due to inhibition of a membrane pump or modification of the receptor's transactivation properties. Using receptor photoaffinity labeling experiments, we were able to show that ARA9 enhances AHR signal transduction by increasing the available AHR binding sites within the cytosolic compartment of the cell. Our evidence suggests that ARA9's effects are related to its role as a cellular chaperone; *i.e.* we observed that expression of ARA9 increases the fraction of AHR in the cytosol and also stabilized the receptor under heat stress.

The AHR<sup>1</sup> is a ligand-activated transcription factor that mediates the biological effects of halogenated dioxins and related compounds (1). In a widely held model of dioxin signal transduction, the AHR is found in the cytosol, in a complex with Hsp90 and a newly discovered protein known as ARA9 (2–4).<sup>2</sup> In the presence of agonist, the AHR translocates to the nucleus, where it binds to its nuclear partner, ARNT. This AHR:ARNT heterodimer is capable of binding DNA and promotes the transcription of a battery of responsive genes including those encoding a number of xenobiotic-metabolizing en-

zymes (5). Hsp90 has been shown to play a role in maintaining AHR in a conformation that can bind ligand with high affinity (6–8). Although ARA9 has been shown to increase AHR function in yeast and mammalian cells, its role in AHR signaling is not understood (7–10).

ARA9 was initially identified in yeast two-hybrid screens, in which the AHR or the hepatitis B virus protein X were used as bait (9–11). Later, it was purified from monkey cells in a complex with the AHR (12). ARA9 contains two notable structural motifs. In its amino terminus, ARA9 contains an FKBP homology domain. This domain shares 28% amino acid sequence identity to FKBP12 (9, 11, 12). However, ARA9 is unable to bind FK506 and does not appear to have peptidyl prolyl isomerase activity<sup>3</sup> (13). In its carboxyl terminus, ARA9 contains three TPRs. TPRs are defined by strings of 34 amino acids that have been shown to play roles in protein-protein interaction (14). This domain structure is similar to that found in the GR-associated immunophilin, FKBP52, which contains two FKBP domains in its amino terminus and three TPRs in its carboxyl terminus (15, 16). In addition to their structural similarities, ARA9 and FKBP52 are found associated to the cytosolic complexes of AHR and the GR or progesterone receptor, respectively (9, 11, 12, 17, 18).

In both mammalian cells and yeast, the presence of ARA9 enhances AHR signaling (11–13). Although ARA9 is capable of directly interacting with the AHR:Hsp90 complex, the mechanism by which it influences receptor signaling is unknown. Our experiments in yeast have shown that heterologous expression of ARA9 increases the maximum response and shifts the dose response of the AHR agonist,  $\beta$ NF, to the left (13). In our laboratory, dose-response curves are typically performed using a LexA or GAL4 DNA binding domain fused to the AHR. The chimeras have been shown to have similar pharmacology to that observed for the full-length AHR:ARNT system<sup>3</sup> (7). Given that such chimeras homodimerize to drive transcription, they also do not require ARNT for signal transduction. This simplifies protocols and allows us to focus on factors that influence the AHR without considering effects on ARNT. In this report, we employ a Gal4-AHRN $\Delta$ 166 chimera that allowed us to assess the functional consequences of ARA9 expression on AHR signaling in mammalian cells.

### MATERIALS AND METHODS

**Strains and Plasmids**—*Saccharomyces cerevisiae* strain L40 (MAT a, *his3200*, *trp1-901*, *leu2-3*, *112*, *ade2*, *LYS2::(lexAop)<sub>4</sub>-HIS3*, *URA3::(lexAop)<sub>8</sub>-lacZ*, *gal80*) was used in all yeast pharmacology experiments (19). Plasmid pBTM116 is a 2 $\mu$  TRP-marked *ADH1*-driven expression vector containing the full-length *Escherichia coli* LexA cDNA, followed by a polylinker for generation of fusion proteins (20). The plasmid pYX242 (Novagen, Madison, WI) is a 2 $\mu$ , *TRP1*-driven, *LEU*-marked expression plasmid (PL609). pBTMAHRN $\Delta$ 166 (PL703), pYXARA9 (PL803), pYXFKBP52 (PL805), pY2NLxC (PL740), pS-

\* This work was supported by the Burroughs Wellcome Foundation and by National Institutes of Health Grants ES05703, T32 CA09135, ES07015, and F32 ES05856. The costs of publication of this article were defrayed in part by the payment of page charges. This article must therefore be hereby marked "advertisement" in accordance with 18 U.S.C. Section 1734 solely to indicate this fact.

‡ To whom correspondence should be addressed: McArdle Lab. for Cancer Research, 1400 University Ave., Madison, WI 53706-1599. Tel.: 608-262-2024; Fax: 608-262-2824; E-mail: bradfield@oncology.wisc.edu.

<sup>1</sup> The abbreviations used are: AHR, aryl hydrocarbon receptor; FKBP, FK506-binding protein; Hsp90, heat shock protein of 90 kDa; UAS, upstream activating sequence; PAGE, polyacrylamide gel electrophoresis; PBS, phosphate-buffered saline;  $\beta$ NF,  $\beta$ -naphthoflavone; DEX, dexamethasone; TAD, transactivation domain; GR, glucocorticoid receptor; TPR, tetratricopeptide repeat; SD, synthetic drop-out; MOPS, 4-morpholinepropanesulfonic acid.

<sup>2</sup> ARA9 was identified and named by three separate groups. It is also known as XAP2, for hepatitis B virus X-activating protein 2, and AIP, for AHR-interacting protein.

<sup>3</sup> L. A. Carver and C. A. Bradfield, unpublished results.

GAHRNΔ166 (PL118), pSGAHRNΔ409 (PL246), pSGARNT (PL278), and pSportAHR (PL65) have been described previously (9, 13, 21, 22). The plasmid pSGVP16TAD was a generous gift of Dr. Peggy Farnham. The full-length ARA9 cDNA expression plasmid, pTarget-ARA9 (PL1326), was constructed by polymerase chain reaction amplification of PL580 with OL824 and OL813 and cloning the amplicon into pTarget (Promega, Madison, WI) (9, 13). pTarget-FKBP52 (PL1360) was created by polymerase chain reaction amplification of full-length FKBP52 with OL963 and OL803 from PL805 and cloning the amplicon into pTarget (13). PL186 is a  $\beta$ -galactosidase expression vector driven by an SV40 promoter. pG5luc (PL1083) is a luciferase reporter driven by multiple GAL4 DNA response elements (Promega).

**Pharmacology in Yeast**—The effects of FK506 on AHR signaling were measured in the *S. cerevisiae* strain L40, as described previously (7). Two days after plasmid transformation, colonies were replica-plated onto 78.5-cm<sup>2</sup> plates that had been prepared with Me<sub>2</sub>SO (0.01%) or 10 nM  $\beta$ NF. Where appropriate, 10  $\mu$ M FK506 was added to the culture medium. The replica plates were then incubated for 2 days at 30 °C. For each dose of  $\beta$ NF, three colonies were suspended in 100  $\mu$ l of Z-buffer (60 mM Na<sub>2</sub>HPO<sub>4</sub>, 40 mM NaH<sub>2</sub>PO<sub>4</sub>, 10 mM KCl, 1 mM MgSO<sub>4</sub>, 35 mM 2-mercaptoethanol), and an aliquot was removed for estimation of cell density by the A<sub>600</sub>. Twenty microliters of the remaining cell suspension was added to 130  $\mu$ l of Z-buffer, 25  $\mu$ l of 0.1% SDS (w/v), and 25  $\mu$ l of CHCl<sub>3</sub>. The suspension was disrupted at high speed for 10 s. Thirty microliters of a 4 mg/ml *o*-nitrophenyl- $\beta$ -D-galactosidase solution was added, and the mixture was incubated for 2–5 min at 30 °C. The reaction was stopped by adding 75  $\mu$ l of 1 M NaCO<sub>3</sub>, the cell debris was removed by centrifugation, and the A<sub>420</sub> was determined.  $\beta$ -Galactosidase units were calculated using the following formula: (A<sub>420</sub>/A<sub>600</sub> of 1/10 dilution of cells  $\times$  volume of culture  $\times$  time of incubation)  $\times$  1,000.

**Tissue Culture and Transient Transfection**—All mammalian cell culture experiments were performed in COS-1 cells that were maintained in Dulbecco's modified Eagle's medium supplemented with 10% fetal bovine serum, penicillin (0.1 unit/ml), and streptomycin (0.1  $\mu$ g/ml). Prior to transfection, cells were washed once with Opti-MEM (Life Technologies, Inc.). Transient transfections were carried out in 35-cm<sup>2</sup> tissue culture dishes with LipofectAMINE (Life Technologies, Inc.) as per the manufacturer's instructions. DNA used in transfections was diluted in Opti-MEM and consisted of 0.2  $\mu$ g of AHR plasmid DNA (or other Gal4 chimeras), 0.2  $\mu$ g of modifier DNA (e.g. ARA9), or an empty expression vector to maintain constant DNA concentration. In addition, 0.2  $\mu$ g of GAL4-UAS luciferase was added as a reporter and 0.2  $\mu$ g of SV40- $\beta$ -gal as a control for transfection efficiency. Following treatment of cells with the lipid/DNA mix, the medium was changed to Dulbecco's modified Eagle's medium plus 10% fetal bovine serum, and the appropriate concentrations of  $\beta$ NF or Me<sub>2</sub>SO (vehicle control) were added. Cells were incubated for 16 h at 37 °C and 6% CO<sub>2</sub> and harvested using Passive Lysis Buffer (Promega). Luciferase units were determined using the luciferase assay system as per the manufacturer's instructions (Promega).

**AHR Preparation from Transfected Cells**—COS-1 cells were maintained and transfected as described above with several minor modifications. Cells were maintained in 10-cm<sup>2</sup> dishes and transfected with a combination of 1.6  $\mu$ g of murine AHR DNA and 1.6  $\mu$ g of modifier DNA per plate. To obtain soluble protein fractions from these transfected cells, the following protocol was employed. Following a 16-h incubation, cells were trypsinized and washed twice with PBS. Cell pellets were resuspended in MDEENG buffer (25 mM MOPS, pH 7.4, 1 mM dithiothreitol, 1 mM EDTA, 5 mM EGTA, 0.02% NaN<sub>3</sub>, 10% glycerol) supplemented with 10 mM Na<sub>2</sub>MoO<sub>4</sub>. To minimize protein degradation, samples were disrupted using a Dounce homogenizer in the presence of a protease inhibitor mixture (Roche Molecular Biochemicals). After disruption, samples were subjected to centrifugation at 14,000  $\times$  g (10 min, 4 °C). An additional centrifugation (100,000  $\times$  g, 60 min, 4 °C) was performed to obtain the soluble fraction (commonly referred to as the "cytosolic" fraction) of cellular protein. Protein concentrations were determined, and samples were diluted to a final concentration of 1 mg protein/ml.

**Photoaffinity Labeling and Western Blot Analysis of the AHR**—The photoaffinity labeling of the AHR was carried out as described previously (23). Briefly, the photoaffinity ligand, 2-azido-3-[<sup>125</sup>I]iodo-7,8-dibromodibenzo-*p*-dioxin, was added to a final concentration of 1 nM into tubes containing 150  $\mu$ g/ml soluble protein. The resulting mixture was incubated for 30 min at 20 °C, followed by a 5-min incubation on ice. Unbound ligand was removed by the addition of a 10% volume of charcoal/dextran (10%/1%, w/v) and incubation on ice for 30 min. The charcoal/dextran containing the unbound ligand was removed by centrifugation (2,000  $\times$  g, 10 min, 4 °C). Cross-linking of the receptor-

ligand complex was accomplished by exposure to ultraviolet light (310 nm, 80 watts, 4 cm) for 30 s, and the supernatant was transferred to a clean tube. Four milliliters of acetone was added, and the mixture was incubated for 16 h at -20 °C. The acetone precipitate was removed by centrifugation (2,000  $\times$  g, 10 min, 4 °C), and the pellet was washed with 90% acetone/H<sub>2</sub>O. The samples were resuspended in electrophoresis sample buffer and run on a 7.5% SDS-polyacrylamide gel (24). Gels were analyzed by autoradiography, and appropriate bands were excised and counted on a Minaxi  $\gamma$ -counter (Packard Instrument Co.). Scatchard analysis was performed using Prism graphing software (San Diego, CA) (25). Three assumptions used in the Scatchard analysis are supported by our previous data. First, free probe was equal to total counts added. Second, total bound was set equal to bound. This assumes that nonspecific binding was negligible after SDS-PAGE (23). Third, the efficiency of labeling was 2% (26). For Western blot analysis, 25  $\mu$ g of protein was separated by SDS-PAGE and transferred to a nitrocellulose membrane. The membrane was probed with the appropriate antibody and developed using a secondary antibody coupled to alkaline phosphatase (22).

**Immunocytochemistry**—COS-1 cells were transfected as described above in dual chambered microscope slides (Nalge Nunc International, Naperville, IL). Following a 24-h incubation, cells were washed twice in 1  $\times$  PBS. Cells were then washed once in methanol (4 °C) and overlaid with methanol (4 °C). Slides were incubated at -20 °C for 15 min. The methanol was then removed, and the slides were washed twice with PBS, followed by a 1-h incubation in blocking buffer (3% bovine serum albumin in PBS) at room temperature with gentle agitation. The BEAR-1 antibody was diluted in blocking buffer and added to slides (1 h, room temperature, with agitation). Slides were washed four times for 5 min each in blocking solution at room temperature and then incubated for 30 min at room temperature in the presence of diluted secondary antibody (fluorescein-conjugated goat anti-rabbit IgG, Jackson ImmunoResearch Laboratories, Inc., West Grove, PA). Slides were then washed four times in PBS for 5 min each, followed by a brief wash in H<sub>2</sub>O. Chambers were removed, and the slides were mounted with Vectashield (Vector Laboratories, Inc., Burlingame, CA). Cells were viewed and photographed using fluorescent microscopy.

**Heat Denaturation of the AHR**—Conditions for these experiments were derived from our previous work (26, 27). Cytosolic extracts from transfected COS-1 cells were prepared as described above. At time 0, the cytosol was diluted to a concentration of 167  $\mu$ g/ml in MDEENG buffer, and a sample was removed to determine the initial binding. To start the heat denaturation, the remaining samples (AHR with and without ARA9) were diluted 1:1 in prewarmed (45 °C) MDEENG buffer. After various times of incubation at 45 °C, 1-ml aliquots were removed and chilled by the addition of 4 ml of MDEENG buffer. One-milliliter aliquots of the chilled samples were then incubated in the presence of 1  $\times$  10<sup>5</sup> DPM of the radioligand, 2-azido-3-[<sup>125</sup>I]iodo-7,8-dibromodibenzo-*p*-dioxin for 30 min at 20 °C. After cooling the samples for 5 min on ice, the samples were mixed with ice-cold charcoal/dextran (10%/1%, w/v) for 30 min to remove excess ligand. The charcoal/dextran containing the unbound ligand was removed by centrifugation (2,000  $\times$  g, 10 min, 4 °C), and 1-ml aliquots of the supernatant were counted on a Minaxi  $\gamma$ -counter (Packard Instrument Co.). Nonspecific binding was determined in parallel samples by the addition of a 200-fold excess of 2,3,7,8-tetrachlorodibenzofuran. Specific binding was calculated by subtracting nonspecific counts from total counts. Curves were generated by plotting the specific binding at each time (B<sub>T</sub>) divided by the specific binding at time 0 (B<sub>0</sub>) versus time in minutes.

## RESULTS

Given the role that the transporter, Pdr5p, has been shown to play in GR signaling and given the similarities between the AHR and GR signaling pathways, we first set out to determine if Pdr5p plays a role in our yeast AHR signaling system. L40 yeast were transformed with pBTMΔ166AHR in the presence of pYXARA9 or the corresponding vector control. The resulting plates were replicated onto SD media with or without 10 nM  $\beta$ NF and/or 10  $\mu$ M FK506. Assessment of  $\beta$ -galactosidase activity indicated that ligand-independent signaling of AHR was stimulated 10-fold in the presence of ARA9 (Fig. 1). The addition of  $\beta$ NF led to an additional 9-fold increase above controls (total 90-fold increase; Fig. 1). Treatment with FK506 had no effect on reporter activity in the absence of  $\beta$ NF and slightly inhibited the response to  $\beta$ NF when ARA9 was present. This

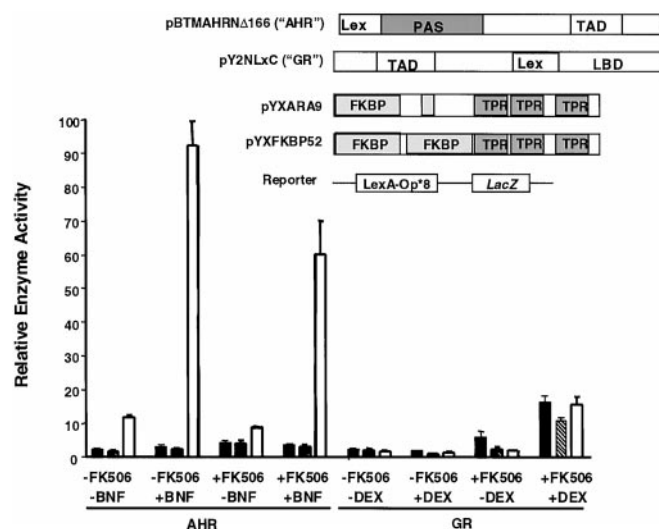


FIG. 1. Effects of FK506 on AHR signaling in yeast. *Top*, schematic diagram of constructs used in yeast transformations. *Bottom*, L40 yeast were cotransformed with pBTMAHR $\Delta$ 166 (AHR, left) or pY2NLx (GR, right). For each receptor chimera, yeast was cotransformed with ARA9 (white bars), FKBP52 (hatched bars), or an empty expression vector (black bars). The resulting transformations were replica-plated onto dishes containing  $\beta$ NF ( $1 \times 10^{-8}$  M) or DEX ( $1 \times 10^{-6}$  M) with and without FK506 ( $1 \times 10^{-5}$  M), as indicated. The yeast was incubated for 48 h and then assayed for  $\beta$ -galactosidase activity from the integrated LexA operator-driven *lacZ* reporter. Each value was normalized by cell number as determined by  $A_{600}$ . Values are expressed relative to the sample that displayed the maximal induction. Error bars represent the S.E. from triplicate determinants. LBD, ligand binding domain.

inhibition was not significant at  $p \leq 0.05$ . As a positive control for FK506 activity as an inhibitor of Pdr5p, the L40 strain was transformed with the GR expression plasmid pY2NLx along with the FKBP52 expression plasmid pYXFKBP52 or the control, pYX242. These experiments were also carried out in the presence or absence of the GR ligand, DEX. We observed that the DEX-induced GR signaling was dependent on the presence of FK506. In the presence of FK506, GR ligand inducibility was 4-fold, and this increase was independent of FKBP52 (Fig. 1).

To analyze the role of ARA9 in AHR signaling in mammalian cells, COS-1 cells were cotransfected with the GAL4- $\Delta$ 166 AHR chimera (pSGAHR $\Delta$ 166), an ARA9 expression vector (pTarget-ARA9), or control plasmid. The transfected cells were then treated with various concentrations of  $\beta$ NF. We observed that the overexpression of ARA9 increased the  $\beta$ NF-driven luciferase expression greater than 4-fold at every  $\beta$ NF concentration tested (Fig. 2). Ligand-independent activation of pSGAHR $\Delta$ 166 was also increased approximately 4-fold in the presence of ARA9.

The ability of ARA9 to influence transactivation was assessed by cotransfecting various GAL4-TAD chimeras (pSGAHR $\Delta$ 409, pSGARNT, pSG424, and pSGVP16TAD) in the presence and absence of pTarget-ARA9. Transfections were normalized to  $\beta$ -galactosidase expression, and the ratio of transactivation activity in the presence of ARA9 to vector control was determined. ARA9 was capable of increasing the activity of pSGAHR $\Delta$ 166 greater than 4-fold. ARA9 did not significantly influence the activity of any other construct including the AHR TAD construct, pSGAHR $\Delta$ 409 (Fig. 3).

The specificity of the effect of ARA9 on AHR was tested by cotransfection with the ARA9 paralogue, FKBP52. We cotransfected pSGAHR $\Delta$ 166 with pTarget-ARA9, pTarget-FKBP52, or the vector control. As shown in Fig. 4A, we observed that FKBP52 was unable to influence pSGAHR $\Delta$ 166 signaling in the presence or absence of  $\beta$ NF. In contrast, ARA9 increased

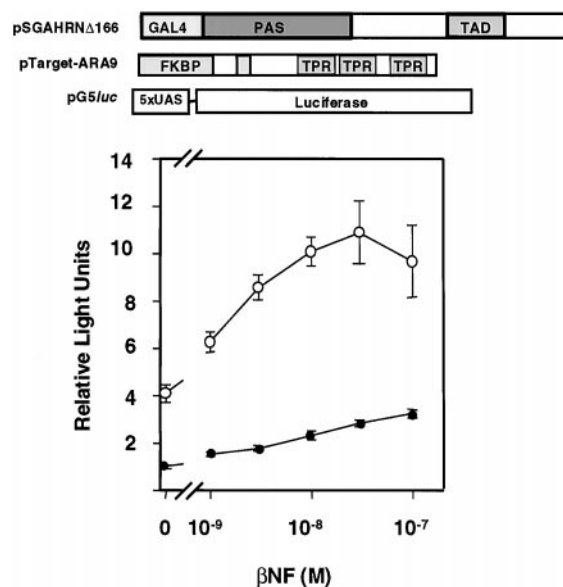


FIG. 2. COS-1 cell transfection with pSGAHR $\Delta$ 166. *Top*, schematic diagram of GAL4-AHR $\Delta$ 166 chimera (pSGAHR $\Delta$ 166), ARA9 expression plasmid (pTarget-ARA9), and GAL4-UAS reporter (pG5luc). *Bottom*, COS-1 cells were transfected with the GAL4-AHR $\Delta$ 166 chimera in the presence of ARA9 (open circles) or an empty expression vector (solid circles). The cells were treated with the indicated amount of  $\beta$ NF for 16 h and harvested by cell lysis. The resulting lysates were assayed for luciferase and  $\beta$ -galactosidase activity. Each value is normalized to its  $\beta$ -galactosidase value to control for transfection efficiency, and all values were normalized within the experiment by setting the control sample in the absence of ligand to a value of 1. Error bars represent the S.E. from triplicate determinants.

activity in both a ligand-dependent and -independent fashion. Expression of ARA9 and FKBP52 in transfected cells was confirmed by Western blot analysis (Fig. 4B).

One possible explanation for the increase in maximal response and leftward shift in the dose-response curve (Fig. 1 and Ref. 13) is that ARA9 is increasing available AHR in these cells. To test this hypothesis, we transfected pSGAHR $\Delta$ 166 in the presence and absence of pTarget-ARA9 in COS-1 cells. Soluble protein fractions were analyzed for their ability to bind the AHR photoaffinity ligand, 2-azido-3-[ $^{125}$ I]iodo-7,8-dibromodibenzo-*p*-dioxin. Saturation binding isotherms indicate that the presence of ARA9 increased the number of ligand binding sites by 2.4-fold (Fig. 5, A and B). Scatchard analysis of these data confirms the increase in binding sites ( $B_{\max} = 2.6 \times 10^{-11} \pm 0.3 \times 10^{-11}$  M for control and  $6.5 \times 10^{-11} \pm 0.2 \times 10^{-11}$  M in the presence of ARA9), with no significant change in  $K_D$  ( $K_D = 1.8 \times 10^{-10} \pm 1.1 \times 10^{-10}$  for control and  $1.5 \times 10^{-10} \pm 0.4 \times 10^{-10}$  in the presence of ARA9) (Fig. 5C).

To extend these results to the full-length AHR, COS-1 cells were cotransfected with a full-length AHR construct (pSporAHR), and pTarget-ARA9 or an empty expression vector. Soluble protein fractions were prepared from the cells, and the AHR was identified by photoaffinity labeling or by Western blot analysis. Using a saturating concentration of photoaffinity ligand, we observed that the presence of ARA9 increased the amount of full-length AHR labeling approximately 2-fold (Fig. 6,  $p \leq 0.05$ ). To determine if ARA9 was increasing the amount of AHR in these soluble extracts, total receptor was estimated by Western blot analysis. Given the qualitative nature of Western blot analysis, multiple independent experiments were performed, and representative results are shown in Fig. 7. These blots show a change in total AHR protein that is consistent with a 2-fold increase. (Fig. 7, A and B). This experiment has been repeated under a variety of conditions with similar results.

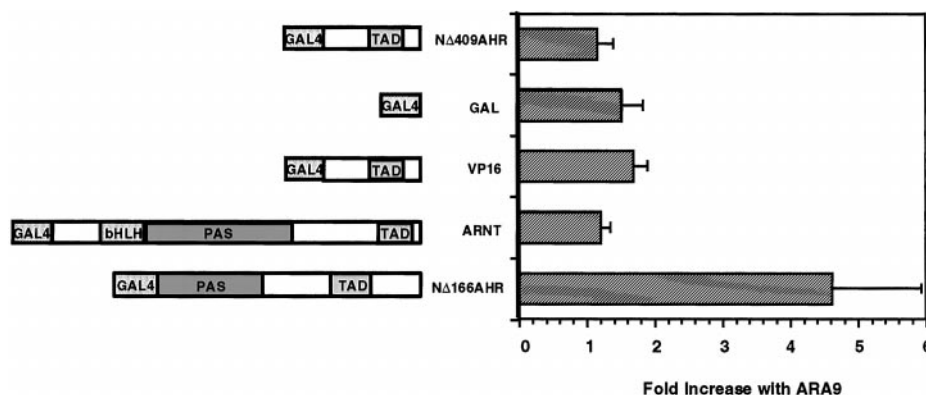


FIG. 3. Cotransfection of ARA9 and various TAD constructs. *Left*, schematic diagrams of GAL4-TAD constructs used in the cotransfections. *Right*, various GAL4-TAD constructs were cotransfected with ARA9 or an empty expression vector into COS-1 cells. Cells were incubated for 16 h and assayed for luciferase and  $\beta$ -galactosidase activity. Each sample was normalized to  $\beta$ -galactosidase activity in the presence of ARA9 over the activity in the presence of empty vector. NΔ166AHR, pSGAHRNΔ166; ARNT, pSGARNT; VP16, pSG-VP16 TAD; GAL, pSG424; NΔ409AHR, pSG AHR NΔ409, which contains the TAD of AHR. Error bars represent the S.E. from triplicate determinants. bHLH, basic helix-loop-helix.

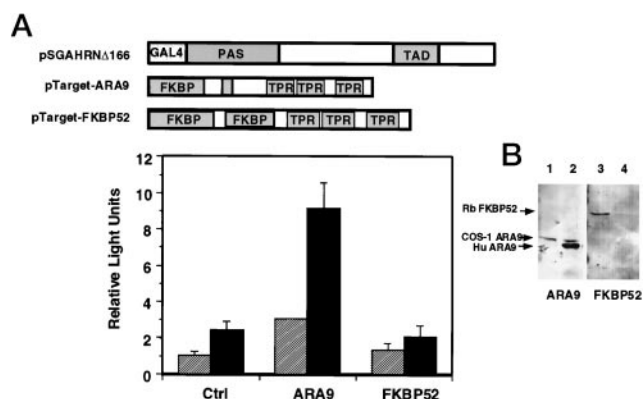


FIG. 4. Cotransfection of pSGAHRNΔ166 and ARA9 or FKBP52. *A* (top), schematic representation of constructs used in transfection. *A* (bottom), COS-1 cells were transfected with pSGAHRNΔ166 (the GAL4-AHRNΔ166 chimera) in the presence of an empty expression vector (*Ctrl*) or ARA9 or FKBP52 expression vectors. Cells were incubated in the absence (*hatched bars*) or presence of  $3.0 \times 10^{-8}$  M  $\beta$ NF (*solid bars*). Cells were assayed for luciferase and  $\beta$ -galactosidase activity. Each value is normalized to its  $\beta$ -galactosidase value to control for transfection efficiency, and all values were normalized within the experiment by setting the control sample in the absence of ligand to a value of 1. Error bars represent the S.E. from triplicate determinants. *B*, Western blot analysis was performed on cytosolic extracts from identical transfections described in *A*. Extracts were prepared as described under "Materials and Methods" and separated on SDS-polyacrylamide gel. Following transfer to nitrocellulose, the blots were probed with antibodies specific for ARA9 (*lanes 1 and 2*) or FKBP52 (*lanes 3 and 4*). Cells transfected with empty vector were used as control (*lanes 1 and 4*). Hu ARA9 is the transfected human ARA9, COS-1 ARA9 is endogenous ARA9, and Rb FKBP52 is transfected rabbit FKBP52.

One possible explanation for the observed increase in total and functional AHR in our soluble fractions was that ARA9 is capable of altering the cellular localization of the AHR in the cell. To test this idea, subcellular localization of the AHR was determined by immunohistochemistry in COS-1 cells that were transfected with pSportAHR in the presence or absence of ARA9 (28). As seen in Fig. 8A, in COS cells, the transiently expressed AHR is found predominantly in the nuclear compartment, with only limited cytoplasmic staining. This expression pattern is shifted to almost completely nuclear in the presence of ligand, demonstrating that the cytosolic fraction of the AHR is functional (Fig. 8A). In the presence of cotransfected ARA9, transiently expressed AHR is almost completely cytosolic. To demonstrate that this receptor is functional, we showed that the addition of agonist leads to translocation of the AHR to the nuclear compartment when ARA9 is expressed.

A second explanation for the increased functional AHR was that ARA9 stabilized the protein against degradation. To test this hypothesis, we transfected pSGAHRNΔ166 in the presence and absence of ARA9 in COS-1 cells. Soluble protein fractions were prepared and heat-stressed at 45 °C for various times. Samples were analyzed by reversible binding, and heat denaturation curves were determined. The coexpression of ARA9 increased the half-life of AHR by almost 2-fold (from 7.9 to 12.8 min) (Fig. 8B).

#### DISCUSSION

Several laboratories have shown that ARA9 is a component of the AHR-Hsp90 complex (9, 11, 12). Our previous work in yeast has shown that ARA9 is capable of modifying AHR signaling by shifting the  $\beta$ NF dose-response curve of AHR to the left and increasing the maximal response (13). Two other laboratories have shown that at a fixed dose of ligand, ARA9 can increase AHR signaling in mammalian cells (11, 12). We undertook this set of experiments to determine how ARA9 may elicit these effects. Several possible mechanisms were considered: 1) that ARA9 influences the amount of free intracellular ligand (29); 2) that ARA9 is acting as a general modifier of the receptor's transactivation properties; and 3) that ARA9 acts by increasing the amount of functional AHR in the cytosol.

Initially, we hoped to draw mechanistic insights into ARA9 function by considering what was known about the role of FKBP52 in steroid receptor signaling. Interestingly, the FKBP52 literature is quite complicated. Despite strong data for a physical interaction between FKBP52 and the GR-Hsp90 complex, there has been no direct evidence that this interaction has any functional consequence. In fact, it now appears that FK506, in the absence of FKBP52, can influence GR signaling by inhibiting an ATP binding cassette transporter, such as Pdr5p (Ref. 29; Fig. 1). Thus, it is plausible that FK506 was influencing cellular pumps by interacting with unknown FK-BPs. Although the chances for this explanation seemed remote, we set out to test the idea that ARA9 could directly inhibit Pdr5p and that this interaction increased the intracellular concentration of the AHR agonist,  $\beta$ NF, in yeast. In effect, we were testing the idea that ARA9 acted like an unknown FK506-FKBP complex that inhibited Pdr5p. As a positive control, we demonstrated that FK506 led to an increase in GR signal transduction in yeast, presumably due to inhibition of Pdr5p (Fig. 1) (29, 30). In contrast, the presence of ARA9 had no influence on DEX-dependent GR signaling, suggesting that ARA9 is incapable of affecting Pdr5p. Also of interest was the observation that FK506 had no influence, or had an inhibitory

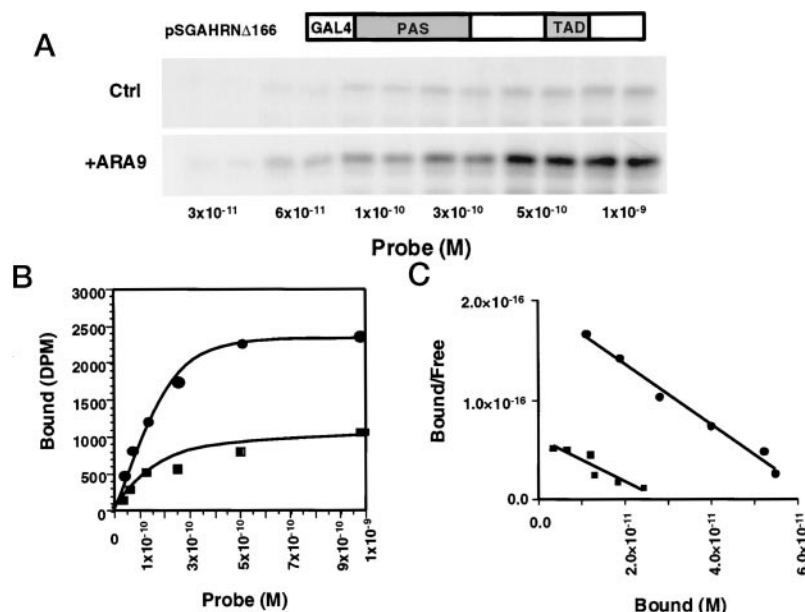


FIG. 5. **Photoaffinity labeling of the GAL4-AHRN $\Delta$ 166 chimera.** *A* (top), schematic diagram of GAL4-AHRN $\Delta$ 166 chimera used in labeling. *A* (bottom), raw data. COS-1 cells were transfected with pSGAHRN $\Delta$ 166 in the presence (+ARA9) or absence (Ctrl) of an ARA9 expression vector. Cytosols were prepared as described under "Materials and Methods." Cytosols were prepared, and photoaffinity labeling was performed in the presence of increasing concentrations of 2-azido-3-[ $^{125}$ I]iodo-7,8-dibromodibenzo-*p*-dioxin. Proteins were separated by SDS-PAGE and visualized by autoradiography. *B*, saturation binding isotherm. Bands corresponding to labeled AHR were excised, counted (*Bound (DPM)*) and plotted as a function of total ligand (*Probe (M)*). Squares, control; circles, with ARA9. *C*, Scatchard analysis. Scatchard analysis was performed on the data from the saturation binding curves as described under "Materials and Methods" (control:  $K_D = 1.8 \times 10^{-10}$  M and  $B_{max} = 2.6 \times 10^{-11}$ ; with ARA9:  $K_D = 1.5 \times 10^{-10}$  and  $B_{max} = 6.5 \times 10^{-11}$ ). Squares, control; circles, with ARA9.

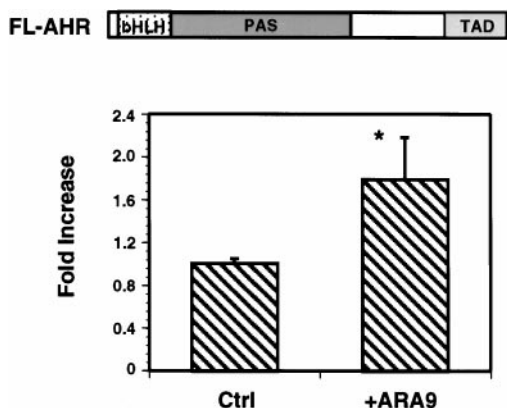


FIG. 6. **Photoaffinity labeling of full length AHR.** *Top*, schematic diagram of full-length AHR construct (*FL-AHR*) used in labeling. *Bottom*, full-length AHR construct was cotransfected with ARA9 (+ARA9) or an empty expression vector (Ctrl). Cytosols were prepared and labeled with 1 nM 2-azido-3-[ $^{125}$ I]iodo-7,8-dibromodibenzo-*p*-dioxin. Proteins were separated by SDS-PAGE and visualized by autoradiography. Bands corresponding to labeled AHR were excised, counted, and plotted (\*,  $p \leq 0.05$ ). Error bars represent the S.D. from triplicate determinants. *bHLH*, basic helix-loop-helix.

effect, on  $\beta$ NF signaling through the AHR. These results demonstrate that the pump, Pdr5p, does not significantly influence intracellular concentrations of  $\beta$ NF.

In our initial experiments, we confirmed that ARA9 had similar effects on AHR signaling in both yeast and mammalian cells. Similar to what we have previously reported in yeast (11), we observed that the cotransfection of ARA9 and AHR in COS-1 cells resulted in an increase in the maximal response and a leftward shift in the dose-response curve of  $\beta$ NF. Interestingly, in both yeast and mammalian cells, ARA9 also increases the background level of AHR signaling (Fig. 2; Ref. 13). There are a number of possible explanations for this. For example, ARA9 could be acting as a ligand for the AHR, or it could be enhancing the response of the AHR to a natural ligand

present in these systems. A conclusion that is consistent with the other data presented in this report is that ARA9 increases the functional levels of the cytosolic AHR by acting as a cellular chaperone. If we assume that some constant fraction of properly folded AHR will be active, then an increase in properly folded AHR, as the result of ARA9 expression, will result in an increase in background activity. Although our data are consistent with this last possibility, we are unable to distinguish between these possibilities, and further experimentation will be necessary to clarify this issue.

To eliminate the possibility that ARA9 was acting as a general modifier of transcriptionally active domains, we also examined its effects on a series of AHR deletion mutants (Fig. 3). In these experiments, we cotransfected ARA9 with various GAL4-TAD chimeras and determined their levels of activity. The results presented in Fig. 3 suggest that ARA9 is not acting at the level of transactivation. Although ARA9 was capable of enhancing the AHRN $\Delta$ 166 construct, it was incapable of increasing the activity of several GAL4-TAD chimeras. Most notably, ARA9 had no effect on the TADs of AHR, ARNT, and VP16. These TAD experiments can also serve as a crude domain map for the AHR interaction surface of ARA9. The observation that ARA9 can influence the AHRN $\Delta$ 166, but not the AHRN $\Delta$ 409, implies that the ability of ARA9 to influence AHR requires amino acids 167–409 (Fig. 3). The observation that this region is also essential for the ability of AHR to physically interact with ARA9 and Hsp90 suggests that the direct interaction is required for ARA9 function (13).

Receptor theory is consistent with the idea that an increase in receptor number can increase the maximal response and create a leftward shift in the dose-response curve (31). Therefore, we performed a number of experiments to determine if ARA9 expression led to an increase in the concentration of the AHR in the "cytosolic" fractions of cells. We first performed a saturation binding analysis on these cellular extracts using the photoaffinity ligand 2-azido-3-[ $^{125}$ I]iodo-7,8-dibromodibenzo-*p*-dioxin. Upon overexpression of ARA9, the number of ligand



FIG. 7. Western blot analysis of transfected AHRN $\Delta$ 166 and full-length AHR in the presence or absence of ARA9. Top, schematic diagram of GAL4-AHRN $\Delta$ 166 chimera and full-length AHR constructs used in transfection. Bottom, A, pSGAHRN $\Delta$ 166 was transfected in the presence of ARA9 (+ARA9) or control vector (Ctrl). Twenty-five micrograms of cytosol was analyzed by Western blot using an antibody specific for the AHR. Bottom, B, full-length AHR was transfected in the presence of ARA9 (+ARA9) or control vector (Ctrl). Twenty-five micrograms of cytosol was analyzed by Western blot using an antibody specific for the AHR. bHLH, basic helix-loop-helix.

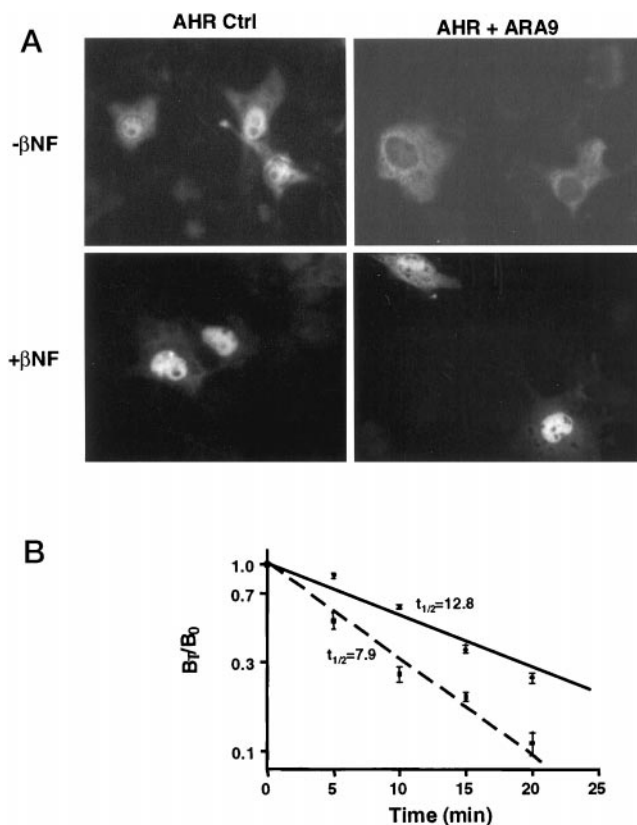


FIG. 8. Immunocytochemistry of AHR and heat denaturation of GAL4-AHRN $\Delta$ 166 chimera. A, COS-1 cells were transfected in the presence or absence of ARA9 and stained with antibodies specific for the AHR as described in the methods. B, pSGAHRN $\Delta$ 166 was transfected in the presence of ARA9 (circles, solid line) or control vector (squares, dashed line). Soluble protein fractions were prepared and subjected to heat stress at 45 °C for various times. Receptor integrity was analyzed by binding assays with 1 nM 2-azido-3-[<sup>125</sup>I]iodo-7,8-dibromodibenzo-*p*-dioxin. Samples were counted and plotted as a described under "Materials and Methods." Error bars represent the S.E. from three separate experiments.

binding sites of the AHR chimera was increased approximately 2.5-fold (Fig. 5). Similar binding results were obtained when using the full-length AHR (Fig. 6). Results from Western blot analysis were also consistent with a 2–3-fold increase in AHR protein levels when ARA9 was cotransfected (Fig. 7). Taken in sum, these results suggest that ARA9 is acting by increasing the amount of available receptor binding sites in the cell's cytosol.

Our data suggest that ARA9 influences AHR levels by more than one mechanism. Immunocytochemistry experiments indicate that ARA9 is acting to maintain the AHR in the cytosolic compartment of the cell and that this plays a role in increasing AHR binding sites (Fig. 8A). To fully appreciate these experi-

ments, it is important to note that when the AHR is transiently expressed in COS-1 cells, much of the unliganded protein is found in the nuclei (Fig. 8A).<sup>4</sup> We suggest that much of the transiently expressed protein may be improperly localized to the nucleus due to improper chaperoning, presumably due to low constitutive levels of ARA9. Our data also suggest that when ARA9 is overexpressed in these cells, a larger fraction of the AHR is properly folded, and it is held in the cytosolic compartment, in a state capable of binding ligand. An ARA9-mediated improvement in AHR folding may also increase cytosolic receptor concentration by a second mechanism; *i.e.* the increase in receptor number may also be related to ARA9's role in stabilizing the AHR from thermal denaturation, thus protecting it from degradation. We examined this by subjecting the AHR to heat denaturation in the presence or absence of ARA9. In this assay, ARA9 was capable of stabilizing the receptor, increasing its half-life at 45 °C by almost 2-fold (Fig. 8B). Given the currently available immunological reagents, it is not possible to determine the relative contributions that ARA9-mediated cellular localization or stabilization make to increasing AHR number *in vivo*. However, it seems likely that each factor is at play. In fact, the effect of ARA9 on AHRs stabilization and subcellular localization may be mechanistically linked.

Taken in sum, these observations support the physiological importance of the AHR-ARA9 physical interaction. In keeping with our previous yeast data, we show that ARA9 is specific for the AHR and that its paralogue, FKBP52, is incapable of affecting AHR signaling in mammalian cells. Our data suggest that ARA9 is not acting by inhibiting the membrane  $\beta$ NF pump; nor is it acting as a general regulator of transcriptional activity. More importantly, we have clearly demonstrated that coexpression of ARA9 and AHR in COS-1 cells results in an approximately 2.5-fold increase in the number of cytosolic AHR binding sites. This increase in functional AHR appears to be due to ARA9's role in receptor folding, yielding a receptor with greater stability and more appropriate subcellular localization in the absence of ligand.

**Acknowledgments**—FK506 was a generous gift of Fujisawa Healthcare Inc. (Ft. Washington, PA). We also thank Dr. Alan Poland for the precursor to the photoaffinity ligand.

#### REFERENCES

- Schmidt, J. V., and Bradfield, C. A. (1996) *Annu. Rev. Cell Dev. Biol.* **12**, 55–89
- Dolwick, K. M., Swanson, H. I., and Bradfield, C. A. (1993) *Proc. Natl. Acad. Sci. U. S. A.* **90**, 8566–8570
- Whitelaw, M. L., Gottlicher, M., Gustafsson, J. A., and Poellinger, L. (1993) *EMBO J.* **12**, 4169–4179
- Fukunaga, B. N., Probst, M. R., Reisz-Porszasz, S., and Hankinson, O. (1995) *J. Biol. Chem.* **270**, 29270–29278
- Whitlock, J. P., Jr., Chichester, C. H., Bedgood, R. M., Okino, S. T., Ko, H. P., Ma, Q., Dong, L., Li, H., and Clarke-Katzenberg, R. (1997) *Drug Metab. Rev.* **29**, 1107–1127

<sup>4</sup> J. J. LaPres, E. Glover, E. E. Dunham, M. K. Bunger, and C. A. Bradfield, unpublished observation.

6. Pongratz, I., Mason, G. G., and Poellinger, L. (1992) *J. Biol. Chem.* **267**, 13728–13734
7. Carver, L. A., Jackiw, V., and Bradfield, C. A. (1994) *J. Biol. Chem.* **269**, 30109–30112
8. Perdew, G. H. (1988) *J. Biol. Chem.* **263**, 13802–13805
9. Carver, L. A., and Bradfield, C. A. (1997) *J. Biol. Chem.* **272**, 11452–11456
10. Kuzhandaivelu, N., Cong, Y.-S., Inouye, C., Yang, W.-M., and Seto, E. (1996) *Nucleic Acids Res.* **24**, 4741–4750
11. Ma, Q., and Whitlock, J. P., Jr. (1997) *J. Biol. Chem.* **272**, 8878–8884
12. Meyer, B. K., Pray-Grant, M. G., Vanden Heuvel, J. P., and Perdew, G. H. (1998) *Mol. Cell. Biol.* **18**, 978–988
13. Carver, L. A., LaPres, J. J., Jain, S., Dunham, E. E., and Bradfield, C. A. (1998) *J. Biol. Chem.* **273**, 33580–33587
14. Lamb, J. R., Tugendreich, S., and Hieter, P. (1995) *Trends Biochem. Sci.* **20**, 257–259
15. Tai, P. K., Albers, M. W., Chang, H., Faber, L. E., and Schreiber, S. L. (1992) *Science* **256**, 1315–1318
16. Renoir, J. M., Radanyi, C., Faber, L. E., and Baulieu, E. E. (1990) *J. Biol. Chem.* **265**, 10740–10745
17. Smith, R. H., Zhao, Y., and O'Callaghan, D. J. (1994) *Virology* **202**, 760–770
18. Pratt, W. B. (1993) *J. Biol. Chem.* **268**, 21455–21458
19. Vojtek, A. B., Hollenberg, S. M., and Cooper, J. A. (1993) *Cell* **74**, 205–214
20. Bartel, P. L., Chien, C., Sternglanz, R., and Fields, S. (1993) in *Cellular Interactions in Development: A Practical Approach* (Hartley, D. A., ed) pp. 153–179, IRL Press, Oxford
21. Dolwick, K. M., Schmidt, J. V., Carver, L. A., Swanson, H. I., and Bradfield, C. A. (1993) *Mol. Pharmacol.* **44**, 911–917
22. Jain, S., Dolwick, K. M., Schmidt, J. V., and Bradfield, C. A. (1994) *J. Biol. Chem.* **269**, 31518–31524
23. Bradfield, C. A., Kende, A. S., and Poland, A. (1988) *Mol. Pharmacol.* **34**, 229–237
24. Poland, A., Glover, E., Ebetino, F. H., and Kende, A. S. (1986) *J. Biol. Chem.* **261**, 6352–6365
25. Scatchard, G. (1949) *Ann. N. Y. Acad. Sci.* **51**, 660
26. Bradfield, C. A., Glover, E., and Poland, A. (1991) *Mol. Pharmacol.* **39**, 13–19
27. Poland, A., Teitelbaum, P., and Glover, E. (1989) *Mol. Pharmacol.* **36**, 113–120
28. Jain, S., and Bradfield, C. A. (1998) *Mech. Dev.* **73**, 117–123
29. Kralli, A., and Yamamoto, K. R. (1996) *J. Biol. Chem.* **271**, 17152–17156
30. Kralli, A., Bohlen, S. P., and Yamamoto, K. R. (1995) *Proc. Natl. Acad. Sci. U. S. A.* **92**, 4701–4705
31. Nickerson, M. (1956) *Nature* **178**, 697